HOSTED BY

National Authority for Remote Sensing and Space Sciences

The Egyptian Journal of Remote Sensing and Space Sciences

www.elsevier.com/locate/ejrs
www.sciencedirect.com

ELSEVIER

CrossMark

RESEARCH PAPER

Extracting and analyzing forest and woodland cover change in Eritrea based on landsat data using supervised classification

Mihretab G. Ghebrezgabher [a,b], **Taibao Yang** [a,*], **Xuemei Yang** [c], **Xin Wang** [a], **Masihulla Khan** [b]

[a] *Institute of Glaciology and Ecogeography, College of Earth and Environmental Sciences, Lanzhou University, Lanzhou 730000, China*
[b] *Eritrea Institute of Technology, College of Education, Mai-Nefhi 12676, Eritrea*
[c] *Gansu Desert Control Research Institute, Lanzhou 730070, China*

Abstract Remote sensing images are suitable for quantifying and analyzing land-cover dynamics, particularly for forest-cover change. In this study, the methodology used the supervised classification technique to classify and analyze the total forest-cover change in Eritrea. The results indicated that the forest and woodland cover extracted with high overall accuracy and kappa coefficient of approximately 96% and 0.94, respectively. Generally, the forest cover declined from 2966 km^2 to 1401 km^2 from the 1970s to 2014, and the woodland forest cover was reduced from 14,879 km^2 to 13,677 km^2 in the same period. The annual rate of deforestation was very high, with approximately 0.35% (62 km^2) of the total forest cover lost each year for the last 44 years. The study concluded that deforestation is one of the leading causes of environmental degradation in the country and it might be caused by human factors as well as due to climate change, i.e., by prolonged drought and inadequate and erratic rainfall. Thus, this paper may significantly help decision makers and researchers who are interested in remote sensing for forest management and monitoring, and for controlling and planning development at local, regional, and global [scales].

1. Introduction

Forest ecosystems cover one-third of the Earth's land surface. They are important resources for nations. Forests play a signif-

icant role in environmental protection, such as soil conservation, increasing biodiversity, and prevention of climate change. Forests are beneficial for long-term national economic growth through providing raw material such as timber for industry and construction, and as a source of medicines. In addition, forests reduce global warming through the carbon cycle and ecosystems (Baumann et al., 2014; Kim et al., 2014). However, the forest resources of the world are

endangered by different human factors. According to Chakravarty (2012), approximately 0.20% of world forest cover was lost between 1990 and 2000 and approximately 0.13% in the next 10 years between 2000 and 2010. In addition, approximately 0.56% of the total forest in Africa was lost between 1990 and 2000, and 0.49% was lost from 2000 to 2010. The highest rate of deforestation occurred in East and Southern Africa, approximately 0.62% and 0.66%, between 1990 and 2000 and 2000 and 2010, respectively. Kim (2014) found that the rate of deforestation was higher in Africa than in any other part of the world, particularly in the Democratic Republic of Congo, with the growth of agro-industries.

In Eritrea, deforestation is one of the most serious environmental problems and it is caused mainly through human activity and climate change. Because approximately 80% of the population depends on farming, the negative impact of shifting and subsistence cultivation and overgrazing on forests is significant, and the dependence on firewood and traditional housing are also factors contributing to deforestation. Effects of climate change include infrequent and uneven distribution of rainfall and prolonged droughts, particularly in the 1960s, 1970s, 1980s, and early 1990s (Hessel et al., 2009; Bobee et al., 2012; Brandt et al., 2014; Waal, 1991), and have contributed significantly to deforestation in the Sahel region, including Eritrea. According to the Ministry of Land, Water and Environment (MLWE), 2012, increase in temperature, which leads to a high rate of evaporation of moisture from the soil, is the main contributing factor for deforestation in Eritrea. According to researchers such as (Nyssen et al., 2004) 30–40% of the total area of the country was covered by forest in the year 1900. Forest currently covers only approximately 13.7% of the country, including the woodland forests (MOA, 2002; Arayal, 1999). The United Nations Food and Agriculture Organization (FAO) reported that the total forest area (including woodland forest) in Eritrea was approximately 15,276 km^2 in 2010. According to the FAO, Eritrea has lost an average of 45,000 and 44,000 hectares of forest every year between 1990 and 2000, and 2000 and 2010, respectively, which annually is a loss of approximately 0.28% (44 km^2), and approximately 89,000 hectares of forest cover was lost within 20 years of independence, from 1990 to 2010.

Advanced technology, such as GIS and remote sensing, which emerged in early 1970s, is vital to the world, particularly to environmental scientists (Jayanth et al., 2015; Brink et al., 2014). Recently, different researchers (Baumann et al., 2014; Chasmer et al., 2014; Churches et al., 2014; Dronova et al., 2015; Iqbal and Khan, 2014; Zhang et al., 2013; Butt et al., 2015; Naqvi et al., 2014) have used remote-sensing data for land-use classification, monitoring, and management of land degradation and quantifying and analyzing land-use changes. Landsat data are also used to investigate land degradation, such as desertification and deforestation. Remote sensing and GIS studies of environmental degradation are more effective than field surveys in terms of cost, time, and area coverage (El Baroudy and Moghanm, 2014). Today, many different scientific approaches, together with remotely sensed satellite images and GIS, play important roles in analyzing and monitoring land-cover change based on time series (Jayanth et al., 2015; Yiran et al., 2012; Huang and Siegert 2006; Rawat and Kumar 2015). However, less-developed countries in Africa, such as Eritrea, are far from the application of these technologies or their use is very limited, although they are valuable

tools for assessing environmental changes in the Sahel region (Brandt et al., 2014). This circumstance might be the result of a lack of access and poor education facilities, especially in Eritrea, because the country is new, the introduction of this technology has been very slow. Particularly, the monitoring and managing of land degradation such as deforestation and desertification with the help of remote-sensing technology and GIS applications is very limited.

Several Landsat data classification methods or techniques enable us to analyze and assess the different land cover types. The most common methods of classification are unsupervised and supervised (Belgiu and Dragut, 2014; Papa et al., 2012). The unsupervised method of classification is independent of external sources. The classification of the image is done automatically and involves random sampling in unknown land-cover types. Accuracy may not be efficient, although it is essential. The supervised method of classification is a dependent method and is more controlled than the unsupervised method. The supervised method requires creating a signature based on the region of interest or on training sites, and then the software runs automatically for the process of classification. Different classification methods can be used, such as parallelepiped, minimum distance, Mahalanobis distance, maximum likelihood, and spectral angler mapper. However, the most commonly used technique is the maximum likelihood to natural nearby-neighbor algorithm (Keuchel et al., 2003). The accuracy of the supervised classification depends on the sampling and the quality of the training data, which is more suitable than the unsupervised method (Yiran et al., 2012; Iqbal and Khan, 2014).

Therefore, the purpose of this paper is to extract and analyze forestland and woodland cover change over the past four decades. To analyse and assess the distribution and change of forest and woodland in Eritrea, we used Landsat data from the 1970s, the 1980s, and 2014. In addition, we used statistical data to evaluate the annual rate of deforestation or loss of total forest cover and predicted forest and woodland cover change in the coming 30 years.

2. The study area

Eritrea is located in arid, semi-arid, and sub-humid parts of the Sahel region in Africa. It is a small country situated on the western side of the Red Sea in East Africa. It is located between 12° 22′ and 18° 02′ N latitude and between 36° 26′ and 43° 13′ E longitude (Teklay, 1999; Nyssen et al., 2004; Ghebrezgabher et al., 2014). Eritrea is bordered by Sudan in the north and west, Djibouti in the southeast, Ethiopia in the south, and the Red Sea in the east (Fig. 1). No consistent data about the size of the country are available, but in this study, the total area of the country is considered to be approximately 125,902 km^2. The country comprises a coastline of approximately 1900 m and approximately 390 islands in the Red Sea.[8] Today, the total population of the country is estimated to be 6.2 million, and approximately 80% of the population are engaged in primary economic activities, such as agriculture, fishing, herding, and forestry (MLWE, 2012).

Eritrea has an elongated shape and comprises a very complex topography of mountains, valleys, rivers, escarpments, highlands, and lowlands. The elevation varies from below sea level in the Danakil depression to above 3000 m in the
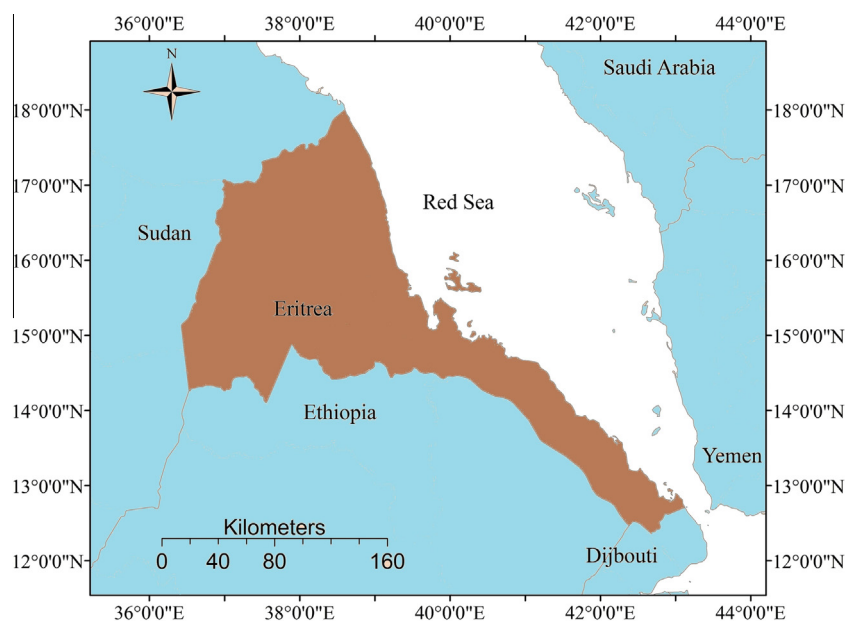
Figure 1 Geographical location of the study area.

southern highland of the country. Eritrea is bounded by the western and eastern lowlands where the highland in between, trends north to south. The highland is a plateau with steep-sided eastern and western escarpments. Thus, the weather and climate of the country are highly influenced by its physical features. Temperature increases from the highlands toward both lowlands. The annual average temperature in the central highland is approximately 16° C in Asmara, the capital city, and 30° C in the western and eastern lowlands in Agordet and along the coast in Massawa, the port city. Rainfall is extremely variable in time and amount. There is no persistent distribution of rainfall, and it increases from north to south in the highland, which annually receives rainfall of approximately 200 mm and 800 mm, respectively. The eastern escarpment receives rainfall twice per year above 900 mm, the eastern lowland along the coast has the lowest rainfall in the country at less than 200 mm, and the western lowland receives approximately 500 mm annually. Currently, Eritrea experiences different environmental problems, such as desertification, deforestation, overgrazing, and soil erosion. Particularly, desertification and deforestation are the most serious land degradations. Desertification in the country is largely caused by human activity and climate change, especially drought (Ghebrezgabher et al., 2014; Nyssen et al., 2004).

3. Data and methodology

3.1. Landsat data selections

For this paper, remotely sensed images were freely downloaded from the United State Geological Survey website. The images were clear of cloud cover. MSS Landsat_1, MSS Landsat_5, and ETM + images, respectively, were downloaded from the 1970s, the 1980s, and 2014. In this study, 43 satellite images were used to cover the whole area, with 13 of the images from the 1970s and 15 images each from the 1980s and 2014. For the 1970s, 8 Landsat images from 1972,

4 from 1973, and 1 from 1975 with 57-m spatial resolution were downloaded. For the 1980s, 11 images from 1987, 2 from 1985, and 1 each from 1984 and 1986 with 60-m spatial resolution were obtained. For 2014, 30-m resolution Landsat_7 images from different months – 7 from April, 6 from June, and 1 each from May and February – were selected. The UTM zone for all images ranges from 36° N to 38° N, and they were scanned at different sun elevations. For this study, the digital elevation model (DEM) was obtained from the Shuttle Radar Topography Mission (SRTM) at (http://gdem.ersdac.js-pacesystems.or.jp/search.jsp).

3.2. Digital image pre-processing

Landsat image pre-prepossessing is necessary for extracting and quantifying meaningful information from remotely sensed data (Iqbal and khan, 2014; Butt et al., 2015; Naqvi et al., 2014). In this study, digital image pre-processing was performed by application of ENVI 4.7 software. Green, red, near-infrared, and short-wave infrared bands, or bands 1, 2, 3, and 4 and 2, 3, 4, and 5, respectively, for Landsat MSS and Landsat_7 or ETM + , were imported, because forest land cover is more sensitive in the near-infrared band. Image calibration, geometrical and atmospheric correction were completed (Torahi and Rai, 2011; Boori et al., 2015). We used a layer-stacking tool to convert the three bands (1, 2, and 3 for MSS and 2, 3, and 4 for ETM +) for each satellite into a single-layer file, and they were mosaicked into a single file for each period. Gap filling was completed by the use of a build mask for Landsat ETM + . The nearest-neighbor resampling method was used in datum WGS84 (Boori et al., 2015). The mosaicked images were projected to UTM zone 37 N and resampled to 30-m spatial resolution. We applied a masking method to resize the images to the desired size of the study area (Petta et al., 2013; Ma et al., 2011), where each image was prepared for different indices' calculation and supervised classification.

3.3. Indices for classification approach

3.3.1. Normalized Difference Vegetation Index

The Normalized Difference Vegetation Index (NDVI) is the most widely used indicator for vegetation distribution. It is sensitive to chlorophyll in vegetation (Barrett et al., 2014; Yang et al., 2014), and has a linear correlation between density and distribution of vegetation (Li et al., 2011). The NDVI is the difference in the wavelength of red and near-infrared bands, and the value ranges from −1 to 1. The highest value of the NDVI indicates forest and the lowest value indicates desert vegetation. In this study, the NDVI is used to understand the distribution of vegetation throughout the study area, which is significant for enhancing the accuracy of forest and woodland classification change (Rawat et al., 2013; Zhang et al., 2013; Li et al., 2014). However, generally, the variation in the NDVI values is very low, particularly in 2014. Thus, NDVI above 0.31 is considered high to very high vegetation cover (Table 1). The NDVI is calculated as

$$NDVI = (NIR − red)/(NIR + red)$$

where, NIR refers to the near-infrared wavelength and red represents the wavelength in the red band.

3.3.2. Vegetation cover proportion

The vegetation cover proportion (VCP) is similar to the NDVI. However, the VCP explains the density of vegetation cover based on the stems, branches, and leaves of the vegetation (Li et al., 2011). The VCP depends on the NDVI maximum and minimum, and the maximum and minimum NDVI represents vegetation NDVI and soil NDVI, respectively (Li et al., 2011; Zhang et al., 2013). The value falls between 0 and 1. In this study, the VCP is adopted to indicate the highest, medium, and lowest vegetation cover throughout the study periods, and it is very significant for maximizing the classification accuracy. In our study, a VCP > 0.64 is considered high to very high vegetation cover (Table 1 and Fig. 2). The VCP is given by the following formula:

$$VCP = (NDVI − NDVI_{min})/(NDVI_{max} − NDVI_{min})$$

where, $NDVI_{max}$ and $NDVI_{min}$ represent vegetation NDVI and soil NDVI, respectively.

3.3.3. Soil Adjusted Vegetation Index

The Soil Adjusted Vegetation Index (SAVI) is used to minimize the effect of brightness reflection in the NDVI, which is caused by the soil. The SAVI is very useful in areas with spare vegetation cover, such as arid and semi-arid regions. According to Huete (1988), the SAVI depends on near-infrared and red bands, with a constant L factor that is added to the denominator of the NDVI formula to adjust for the effect of soil. The

SAVI value ranges from −1 to 1. However, it should be multiplied with the numerator by $1 + L$, because the NDVI value ranges between −1 and 1 (Huete, 1988; Gilabert et al., 2002; Aggarwal and Minz, 2013). The L factor is 0.5 for a very spare canopy of vegetation, 1 for a medium canopy of vegetation, and 0 for a very high canopy of vegetation. In this study, the SAVI is important because more than 70% of the country is arid and semi-arid (MLWE, 2012), and the distribution of the NDVI value is generally very low, particularly in 2014, except in a few areas/pixels. Thus, we applied 0.5 as constant factor (L) to all pixels, except some pixels under high forest cover, where the L factor was zero and the SAVI > 0.68 generally falls under high vegetation cover (Table 1). SAVI is defined as

$$SAVI = (NIR − red) * 1 + L/(NIR + red + L)$$

where, NIR is near-infrared band, red refers to the red band, and L is the constant factor.

3.3.4. Modified/Normalize Difference Water Index

McFeeter (1996) introduced the Normalized Difference Water Index (NDWI) for analyzing and understanding the location and distribution of water bodies in a particular region. The NDWI is computed from the green and near-infrared bands. However, Xu (2006) first presented the Modified Normalized Difference Water Index (MNDWI) to separate water from land boundary more accurately than the NDWI. Therefore, in this study, we used the NDWI in the MSS image for the 1970s, which lacks the short-wave infrared. Although, no significant water bodies are in the study area, it comprises the longest coastline along the Red Sea. Therefore, the MNDWI might be important for a clear understanding of the distribution of water bodies and also helps minimize misclassifications. According to Xu (2006), the MNDWI depends on the green band and the short-wave infrared band. Recently, several researchers (El-Asmar et al., 2013; Aggarwal and Minz, 2013; Zhang et al., 2013; Li et al., 2011, 2014) have used the MNDWI in their studies. The value for the MNDWI varies from −1 to 1, and the highest value indicates water and the low MNDWI value indicates forest or high vegetation cover. In this study, MNDWI > 0.18 indicates water. The MNDWI is explained by the following formula:

$$NDWI = (Green − NIR)/(Green + NIR) \text{ or}$$

$$NDWI = (Green − SWIR_1)/(Green + SWIR_1)$$

where, Green is a band in the green wavelength, NIR is a band in the near-infrared wavelength, and $SWIR_1$ represents short-wave infrared.

3.4. Image classification processing

The study of land classification in Eritrea is very limited, and the information is not clear and detailed. However, the FAO plays a significant role in classifying the country into different land use types, and we used this classification as a reference. According to the FAO's Forest Resources Assessment (FRA, 2010) for Eritrea, based on the country's land use classification, forest, woodland, and shrub land are defined in Table 2. Therefore, in this study, we used the forest cover map of Eritrea from the FAO (2000), forest classification

Table 1 Summary of the values of vegetation indexes for high to very high, medium, and low to very low vegetation cover and its distribution with DEM.

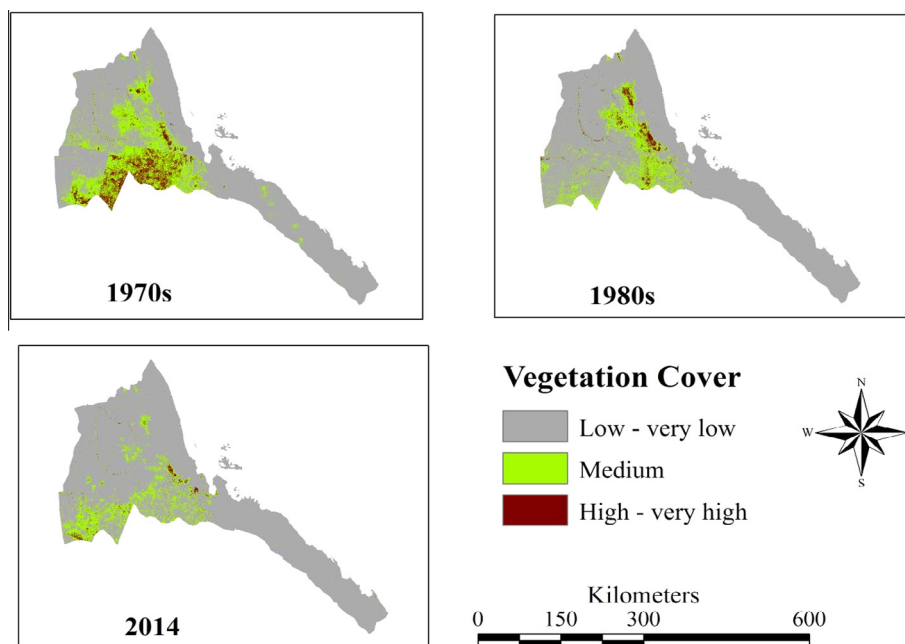| Vegetation cover	NDVI	VCP	SAVI	DEM (m)
High–very high	> 0.31	> 0.64	> 0.68	> 1500
Medium	0.21–0.31	0.58–0.68	0.51–0.68	600–1500
Low–very low	< 0.21	< 0.58	< 0.51	< 600

Figure 2 Distribution of vegetation cover based on VCP in the 1970s, the 1980s, and 2014.

Table 2 Land-use classes based on FAO's FRA 2010.

S. No.	Class	Description
1	Forest	Vegetation or tree cover more than 5 m in height with more than two species, and the canopy or crown ranges from 10% to 40% for open forest and above 40% for closed forest and the forest includes the riverine and mangrove
2	Woodland	Vegetation (trees) composed of one or two tree species with mean height of above 5 m and the canopy cover ranges from 10% to 40% for open woodland and above 40%
3	Shrub land	Shrub land includes the bare soil with sparse vegetation or tree cover and some seasonal grasses, with the vegetation height not more than 5 m and the canopy ranges above 10% for scattered woody land and less than 10% for grassland and wooded grassland
4	Water	Coast water, rivers, streams, wells, channels, and dams

(http://www.fao.org/forestry/country/18314/en/eri/), which was extracted from the global forest cover map, where the country's land cover was classified into closed forest, open/fragmented forest, woodland, other land cover, and water. However, we classified the land cover into forest (open, closed, riverine, and mangrove), woodland forest (open and closed), and other land covers (shrub land, grassland, wooded grassland, scattered woody trees, barren land, cropland, and others), and rivers, streams, artificial reservoirs, and other water bodies are classified as water. We preferred the FRA 2000/11 and 2010 because this classification system has consistency and accuracy and the classification and statistical data published by the FAO, the FRA 2010, are useful to compare and contrast with our data (Churches et al., 2014).

In this study, we adopted the supervised method of classification with maximum likelihood natural nearby neighbor, which is the most commonly used method of classification in remote sensing (Churches et al., 2014; Barrett et al., 2014). Training sites were created on the basis of field work in the most recent year (2014). However, field work is usually limited because of time, cost, and difficulty of reaching some places. Therefore, the above indexes (NDVI, VCP, SAVI, and NDWI

or MNDWI) and a Google Earth map were used to develop and control our signatures and the accuracy of our classification. Generally, forest and woodland forest are located, respectively, between high and very high and medium and high vegetation covers. In this research, approximately 401 pixels/samples were collected to produce signatures, and 100, 102, 170, and 29 samples were selected, respectively, for forest, woodland, other land, and water. We generated the same signatures for 1970s and 1980s satellite images to extract each land use type to avoid biases. Once each site was identified in the combined image, we sketched signatures in each Landsat image for supervised classification using the maximum likelihood classification method.

3.5. Classification accuracy assessment

The classification accuracy assessment is significant for analyzing and evaluating remotely sensed land use/cover data. It has been recently used by many researchers to assess the accuracy of their classification studies (Zhang et al., 2013; Yang et al., 2014; Comber et al., 2012; Rawat et al., 2013; Barrett et al., 2014; Baumann et al., 2014; Churches et al., 2014). Several

methods are applied to measure the accuracy of classification, such as the cross-tabulation method, the confusion matrix, and the generation of random samples (Baumann et al., 2014; Belgiu and Dragut, 2014; Churches et al., 2014). In this study, we implemented the confusion matrix (error matrix) by use of ground truth region of interest (ROI) based on the 401 pixels referenced with the help of ENVI 4.7. The matrix computes the accuracy of each class directly (Ji and Niu, 2014). Thus, the statistical value of the overall accuracy, kappa coefficient, omission error (producer's accuracy), and commission error (user's accuracy) were computed for the 1970s, the 1980s, and 2014. The kappa statistics showed the probability of an agreement that could be expected to present by chance (Yuan et al., 2005), where the value ranges from $+1.0$ to -1.0. On the other hand, it ranges, respectively, from strong agreement to poor agreement (Waal, 1991).
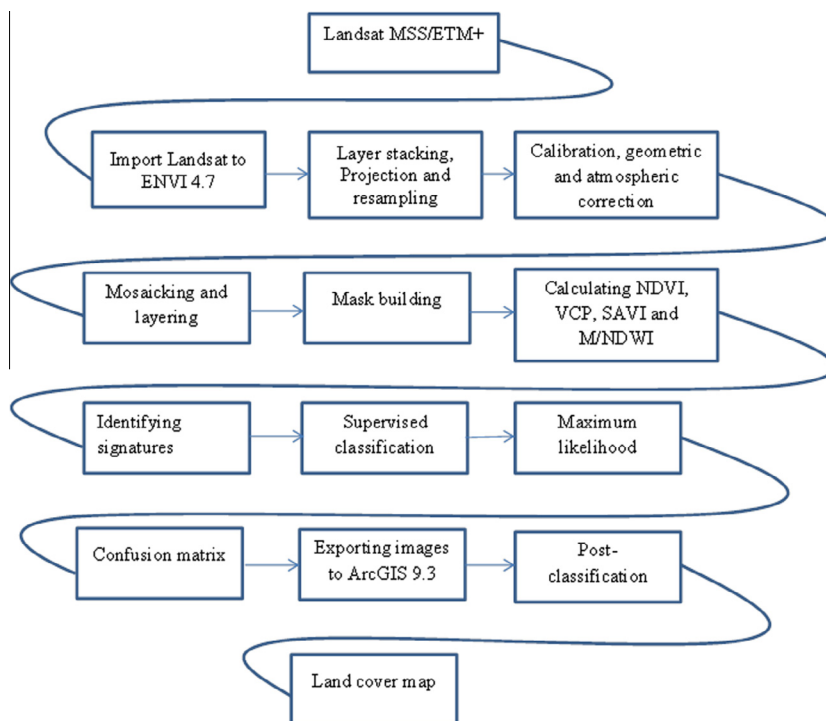
3.6. Classification post-processing

Image post-processing is one of the most important methods used to analyze and evaluate the remotely sensed data. It is implemented by computing the land use change in the different periods (Yuan et al., 2005; Ghebrezgabher et al., 2014). The Landsat images and the DEM were exported from the ENVI 4.7 software to ArcGIS 9.3 for further analysis, where the land-use/cover change for each period was computed from the pixels. The confusion matrices were also exported to a table function (Excel) for further analysis and interpretation. The statistical value of overall accuracy, kappa coefficient, and omission and commission errors were calculated to evaluate the classification accuracy (Foody, 2002). The annual rate of deforestation in each period between the 1970s–1980s, 1980s–2014, and 1970s–2014 were analyzed and evaluated,

and the annual rate of deforestation was expressed either in rate (area/time) or in percentage (Puyavaud, 2003; Tucker and Townshend, 2000). Fig. 3 is the flow diagram for the image processing.

4. Results and discussion

4.1. Land classification change analysis

The study area was classified and quantified into forest, woodland, other lands, and water by use of the supervised technique of classification with maximum likelihood, and the result demonstrated that the forest and woodland cover declined from the 1970s to 2014. The result in Fig. 4 and Table 3 reveals that other lands were the dominant land cover in the east, northeast, and southeast and in the west, northwest, and some parts of the southwest, and in the highlands, covering approximately 87.72% of the region in 2014. Forestland occupied the smallest portion of the region, which was predominantly situated on the eastern escarpment of the country. A small portion of forest cover was also found in the central and southern highlands, along the largest rivers, and in the southwestern region of the country. Forestland covered approximately 2.37% and 1.12%, respectively, in the 1970s and 2014, and the woodland forest was located mostly in the highlands and in a large portion of the southwestern region, where the area coverage decreased from 14,879 km^2 in 1970s to 13,677 km^2 in 2014. The result (Table 3) revealed that the woodland cover was reduced throughout the study period from 11.89% to 10.93% in the past four decades. In the 1970s, approximately 2966 km^2 of the total area was covered by forestland, which declined to 1401 km^2 in 2014. Generally, deforestation was a serious environmental problem in all regions of the country.

Figure 3   Flow chart for Landsat image processing.
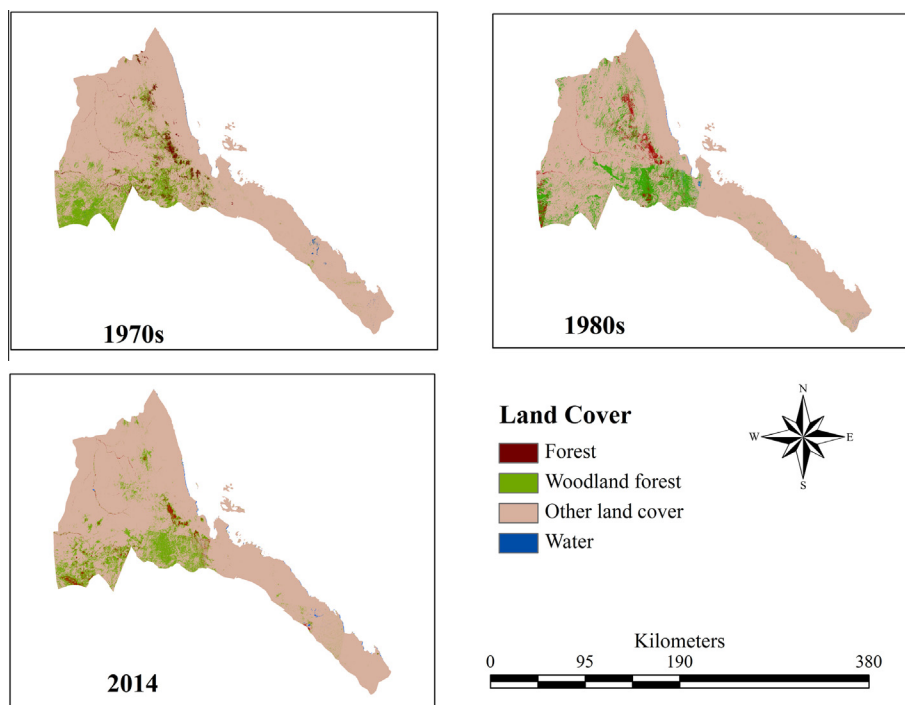
Figure 4 Supervised classifications of remote-sensing images of forest, woodland, and other land in Eritrea in the 1970s, the 1980s, and 2014.

Table 3 Summary of each land-cover change in km² and percentage from the 1970s to 2014.

Category	1970s		1980s		2014	
	Area (km²)	%	Area (km²)	%	Area (km²)	%
Forestland	2966	2.37	2646	2.12	1401	1.12
Woodland forest	14879	11.89	14465	11.56	13677	10.93
Other land	106890	85.45	107682	86.08	109725	87.72
Water	357	0.29	298	0.24	289	0.23

4.2. Classification accuracy assessment

In this study, the forest and woodland cover change were extracted with high average kappa, and overall accuracy was approximately 0.94 and 96%, respectively. Table 4 illuminates the confusion matrix with user, producer, and overall accuracies and the kappa statistics in percentage for the 1970s, the 1980s, and 2014. Approximately 90% and 98%, 97% and 89%, and 95% and 89% were classified, respectively, as forest and woodland forest in the 1970s, the 1980s, and 2014. Generally, an average of 94% of the study area was extracted correctly as forest area and an average of 91% as woodland forest, and the highest classification accuracy observed in the water area and other land type, respectively, was approximately 98% and 99% as an average. Generally, the overall classification accuracy was under strong or perfect agreement.

4.3. Land cover change detection

Table 5 shows the annual rate of land cover change in square kilometers and percentage between the 1970s and the 1980s,

the 1980s and 2014, and the 1970s and 2014. The result revealed that forest and woodland forest lost throughout the study period because of deforestation were approximately 1.25% (1565 km²) and 0.96% (1202 km²), respectively; forestland and woodland forest were lost in the past four decades; and the highest forest and woodland forest loss, respectively, approximately 1245 km² and 788 km², was observed between the 1980s and 2014. Deforestation was also significant between the 1970s and 1980s, when approximately 734 km² (0.58%) of total forest was lost. Generally, approximately 2.21% (2767 km²) of total forest was lost in the past 44 years. The loss of forest and woodland forest land cover means large areas were converted to shrub lands, which expanded by approximately 2.27% (2835 km²) from the 1970s to 2014. Water area decreased by approximately 0.05% and 0.01%, respectively, between the 1970s and the 1980s, and the 1980s and 2014. Generally, water area decline observed from the 1970s to 2014 was approximately 0.06%.

Table 6 shows the annual rate of deforestation for woodland forest and the evergreen forest, where the highest rate of deforestation observed from the beginning of the 1980s to the end of 2014, for approximately two decades

Table 4 Land-cover change confusion matrix with ground truth ROI (pixels) and user, producer, and overall accuracies with kappa for the 1970s, the 1980s, and 2014.

Class	Forest	Woodland forest	Other land	Water	Total	User Accuracy (%)
1970s						
Forest	90	9	0	0	99	91
Woodland forest	10	91	0	0	101	90
Other land	0	2	170	0	172	99
Water	0	0	0	29	29	100
Total	100	102	170	29	401	
Producer accuracy	90	89	100	100		
Overall accuracy = 95% Kappa = 0.92						
1980s						
Forest	98	0	1	0	99	99
Woodland forest	2	97	2	0	101	96
Other land	0	3	167	1	171	98
Water	0	2	0	28	30	93
Total	100	102	170	29	401	
Producer accuracy	98	95	98	97		
Overall accuracy = 97% Kappa = 0.96						
2014						
Forest	97	5	0	0	102	95
Woodland forest	3	91	1	0	95	96
Other land	0	6	169	1	176	96
Water	0	0	0	28	28	100
Total	100	102	170	29	401	
Producer accuracy	97	89	99	97		
Overall accuracy = 96% Kappa = 0.94						

was, respectively, approximately (51.88 km^2 y^{-1}) and (32.83 km^2 y^{-1}). The rate of deforestation was also significant between the end of the 1970s and the 1980s, when approximately 0.54% (16 km^2 y^{-1}) and 0.14% (20.70 km^2 y^{-1}), respectively, for forest and woodland forest were recorded. Generally, approximately 1.20% (35.57 km^2 y^{-1}) and 0.18% (27.32 km^2 y^{-1}) of forest and woodland, respectively, were lost from the 1970s to 2014. Annually approximately 62.89 km^2 (0.35%) of total forest (including woodland forest) was lost in the past 44 years, and the highest rate of total deforestation, approximately 84.71 km^2 y^{-1}, appeared between the 1980s and 2014.

Land cover change classification assessment and analysis from remotely sensed images is the most useful technique since the development of satellite images in the 1970s, when it became more complex and increased its reliability and certainty with continuous advancement in remote-sensing technology. In this study, we have extracted and quantified the historical forest and woodland forest change for the 1970s, the 1980s, and 2014 from Landsat MSS and ETM+ images. The result demonstrates that deforestation is a serious environmental problem in the country, where approximately 2767 km^2 of total forest area (including woodland forest) was lost in the

past four decades. However, the use of remote-sensing technology in land use classification in Eritrea and in the Sahel region[4] is limited, particularly in forest or deforestation change analysis. This limited use may be the result of a lack of access to remote-sensing technology, and consequently the knowledge of it is very low. Thus, it is difficult to compare our result with others.

Therefore, as discussed in the paper the forest and woodland forest cover change was extracted with high accuracy using the supervised method of classification with maximum likelihood natural neighbor. Although it is difficult to evaluate the accuracy of classification with the reality or with the actual features on the ground, constructing matrix errors may minimize the misclassification that could occur from clustering of spectral pixels during the classification process. A confusion matrix is one of the most commonly used methods of classification accuracy assessment, but it may not always represent the reality (Chasmer et al., 2014; Shan-long et al., 2006), because the accuracy might be affected by different factors. The different vegetation indexes (NDVI, VCP, SAVI, and MNDWI) used in this paper were also helpful in enhancing the accuracy of the classification, generally based on the

Table 5 Summary of land-cover change in square kilometers and percentage. Negative number indicates area lost.

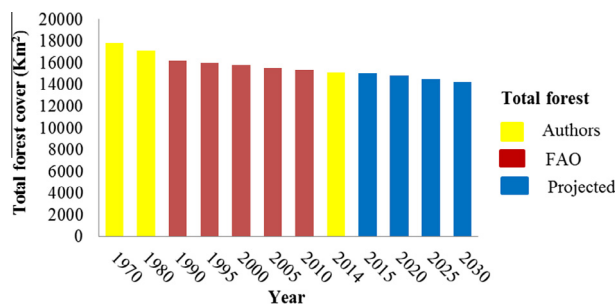| Land cover	1970s–1980s		1980s–2014		1970s–2014	
	Area change (Km^2)	Area change (%)	Area change (Km^2)	Area change (%)	Area change (Km^2)	Area change (%)
Forestland	−320	−0.25	−1245	−1.00	−1565	−1.25
Woodland forest	−414	−0.33	−788	−0.63	−1202	−0.96
Other lands	792	0.63	2043	1.64	2835	2.27
Water	−59	−0.05	−9	−0.01	−68	−0.06

Table 6 Rate of deforestation in square kilometers and percentage (1970s–2014).

Year	Forest		Woodland forest		Total forest	
	km^2y^{-1}	%	km^2y^{-1}	%	km^2y^{-1}	%
1970s–1980s	16	0.54	20.70	0.14	36.70	0.21
1980s–2014	51.88	1.96	32.83	0.23	84.71	0.50
1970s–2014	35.57	1.20	27.32	0.18	62.89	0.35

Figure 5 Total forest-cover change (including woodland forest) in the 1970s, the 1980s, and 2014, the total forest cover from the FAO, (1990–2010), and the projected forest cover (2020–2030) in Eritrea.

DEM, low – very-low, medium, and high – very-high vegetation cover were, respectively, located below 600 m, between 600 and 1500 m, and above 1500 m. Therefore, in this study, a limitation might have occurred in the accuracy of the classification, which is affected by the spatial resolution and topography of the study area. The Landsat images used in this study have 30-m resolution, which is relatively low for use in detailed land-use classification (Iqbal and khan, 2014). In addition, the accuracy may be affected by the shadows produced by mountain slopes, especially for water, on the southeastern escarpment of the country, where the landscape is highly rugged and mountainous topography, or in the satellite scene with path/raw 168/050 and 169/050.

Generally, forest loss was very significant throughout the study period from the early 1970s to the end of 2014. The forest and woodland forest cover of approximately 2.37% and 11.89% in the 1970s was reduced to 1.12% and 10.93%, respectively, in 2014. The annual rate of deforestation, or forest area lost, was significant over the study period, and our result is consistent with Ghebrezgabher et al. (2014) and the FAO, 2010. In this study, the result revealed that annually approximately 63 km^2 (0.35%) of total forest was lost from the 1970s to 2014, comparatively higher than the annual rate of deforestation, and approximately 44 km^2 (0.28%) of the total forest lost between 1990 and 2010 (FAO, 2010). Economic and ecological activities are the most common causes of land-cover change (Sexton et al., 2013). In this study, deforestation was relatively high along roads and rivers, and at the top and bottom of some ridges (Ghebrezgabher et al., 2014) and was mainly caused by human activities. However, forest loss might be intensified by climate change, such as drought and inadequate rainfall. In Eritrea, deforestation is commonly caused by anthropogenic factors, such as cutting trees or forest for different purposes, including traditional farming practice, timber, fuel wood, traditional houses (Hidmo) particularly around the 1970s/80s, population growth and urbanization, and a border conflict with the neighboring country (Ethiopia) (MOA, 2002; Waal, 1991; Arayal, 1999; Ghebrezgabher et al., 2014). In addition, deforestation may be caused by climate change, including drought, mainly the prolonged drought during the 1970s and 1980s, and infrequent, uneven, and erratic distribution of rainfall (MOA, 2002). The selling of live trees in the market during drought periods, particularly the drought period between 1989 and 1991, severely damaged the forestland (Waal, 1991). However, the conservation program of afforestation and reforestation has been conducted by the government, which involves students and the community during summer through the Warsay Ykalo campaign (MOA, 2002; Ghebrezgabher et al., 2014). This might play a significant role in restoring the forest area and decreasing the annual rate of deforestation. Fig. 5 shows the total forest cover change from the 1970s, the 1980s, and 2014 based on our study, the statis-

tical value of the total forest of the country estimated by the FAO from 1990 to 2010, and the projected value of total forest cover from 2015 to 2030. According to the FAO (2010), the rate of deforestation is nearly constant at approximately 44 km^2 y^{-1}or 220 km^2 y^{-5}, and the rate of deforestation for this study is approximately 63 km^2 y^{-1} or 315 km^2 y^{-5}. Therefore, we applied the average rate of deforestation (53 km^2 y^{-1} or 265 km^2 y^{-5}) to predict the future forest cover from the total forest cover recorded by the end of 2014. According to Fig. 5, if the annual rate of deforestation and other factors remain constant, the total forest cover would be approximately 14,760, 14,495, and 14,230 km^2, respectively, by the end of 2020, 2025, and 2030.

5. Conclusion

This research uses the supervised approach to extract and analyze the land cover lost in forest and woodland forest in Eritrea based on time series Landsat data. The study demonstrated that deforestation or forest area lost is a very serious environmental concern in the country, where approximately 2767 km^2 (21%) of total forest cover has been lost (including woodland forest) in the past 44 years. The methodology extracted the forest cover with high accuracy where approximately 62 km^2 forest cover was lost annually from the 1970s to 2014. Although the figure for the annual rate of deforestation is different from others, the result is consistent with the FAO's reports of deforestation and forest cover, in which the annual rate of deforestation is very high and serious. Anthropogenic activities might be the main factors of deforestation in the country, such as subsistence cultivation, gathering fire wood, cutting timber, urbanization, road construction, and overgrazing. Climate change, such as prolonged drought might also intensify deforestation, for which high population growth might be the main reason. In this study, the annual rate of deforestation had a decreasing trend that might be the result of the implementation of afforestation, reforestation, and soil-conservation methods by the government and communities. This study may be useful as input data for further studies at local, regional, or global scales.

References

Aggarwal, H.K., Minz, S., 2013. Change detection using unsupervised learning algorithms for Delhi, India. Asia J. Geoinform. 13 (4), 11–15.

Arayal E., 1999. Review of the Existing Studies Related to Fuelwood and/or Charcoal. Forestry Section, Forestry and Wildlife Division, Department of Land Resources and Crop Production, (pp. 5-6), Asmara, Eritrea ftp://ftp.fao.org/docrep/fao/004/X6788E/X6788E00.pdf.

Barrett, B., Nitze, I., Green, S., Cawkwell, F., 2014. Assessment of multi-temporal, multi-sensor radar and ancillary spatial data for grasslands monitoring in Ireland using machine learning approaches. Remote Sens. Environ. 152, 109–124.

Baumann, M., Ozdogan, M., Wolter, P.T., Krylov, A., Vladimirova, N., Radeloff, V.C., 2014. Landsat remote sensing of forest windfall disturbance. Remote Sens. Environ. 143, 171–179.

Belgiu, M., Dragut, L., 2014. Comparing supervised and unsupervised multiresolution segmentation approaches for extracting buildings from very high resolution imagery. ISPRS J. Photogramm. Remote Sens. 96, 67–75.

Bobee, C., Ottle, C., Maignan, F., Ducoudre, N., Maugis, P., Lezine, A.M., Ndiaye, M., 2012. Analysis of vegetation seasonality in Sahelian environments using MODIS LAI, in association with land cover and rainfall. J. Arid Environ. 84, 38–50.

Boori, M.S., Voženílek, V., Choudhary, K., 2015. Land use/cover disturbance due to tourism in Jeseníky Mountain, Czech Republic: a remote sensing and GIS based approach. Egypt. J. Remote Sens. Space Sci. 18, 17–26.

Brandt, M., Romankiewicz, C., Spiekermann, R., Samimi, C., 2014. Environmental change in tine series – an interdisciplinary study in the Sahel of Mali and Senegal. J. Arid Environ. 105, 52–63.

Brink, A.B., Bodart, C., Brodsky, L., Defourney, P., Ernst, C., Donney, F., Lupi, A., Tuckova, K., 2014. Anthropogenic pressure in East Africa-Monitoring 20 years of land cover changes by means of medium resolution satellite data. Int. J. Appl. Earth Obs. Geoinf. 28, 60–69.

Butt, A., Shabbir, R., Ahmad, S.S., Aziz, N., 2015. Land use change mapping and analysis using Remote Sensing and GIS: A case study of Simly watershed, Islamabad, Pakistan. Egypt. J. Remote Sens. Space Sci. 18, 251–259.

Chasmer, L., Hopkinson, C., Veness, T., Quinton, W., Baltzer, J., 2014. A decision-tree classification for low-lying complex land cover types within the zone of discontinuous permafrost. Remote Sens. Environ. 143, 73–84.

Churches, C.E., Wampler, P.J., Sun, W., Smith, A.J., 2014. Evaluation of forest cover estimates for Haiti using supervised classification of Landsat data. Int. J. Appl. Earth Obs. Geoinf. 30, 203–216.

Comber, A., Fisher, P., Brunsdon, C., Khmag, A., 2012. Spatial analysis of remote sensing image classification accuracy. Remote Sens. Environ. 127, 237–246.

Dronova, I., Gong, P., Wang, L., Zhong, L., 2015. Mapping dynamic cover types in a large seasonally flooded wetland using extended principal component analysis and object-based classification. Remote Sens. Environ. 158, 193–206.

El-Asmar, H.M., Hereher, M.E., El-Kafrawy, S.B., 2013. Surface area change detection of the Burullus Lagoon, North of the Nile Delta, Egypt, using water indices: a remote sensing approach. Egypt. J. Remote Sen. Space Sci. 16, 119–123.

El Baroudy, A.A., Moghanm, F.S., 2014. Combined use of remote sensing and GIS for degradation risk assessment in some soils of the Northern Nile Delta, Egypt. Egypt. J. Remote Sen. Space Sci. 17, 77–85.

FAO, 2000. Natural forest formation, Eritrea, forest cover map. Forest Resources Assessment (FRA). Food and Agriculture Organization of the United Nations http://www.fao.org/forestry/country/18314/en/eri/.

FAO, 2010. Country Report Eritrea, Global Forest Resources Assessment (FRA). Food and Agriculture Organization of the United Nations, FRA2010/063, Rome.

Foody, G.M., 2002. Status of land covers classification accuracy assessment. Remote Sens. Environ. 80, 185–201.

Ghebrezgabher, M.G., Yang, T., Yang, X., 2014. Remote Sensing and GIS analysis of deforestation and desertification in central highland and eastern region of Eritrea (1972–2014). Int. J. Sci.: Basic Appl. Res. (IJSBAR). 18 (2), 161–176.

Gilabert, M.A., Gonzalez-Piqueras, J., Garcia-Haro, F.J., Melia, J., 2002. A generalized soil-adjusted vegetation index. Remote Sens. Environ. 82, 303–310.

Hessel, R., Berg, J.V., Kabore, O., Kekem, A.V., Verzandovoort, S., Dipama, J.M., Diallo, B., 2009. Linking participatory and GIS-based land use planning methods: a case study from Burkina Faso. Land Use Policy 26, 1162–1172.

Huang, S., Siegert, F., 2006. Land cover classification optimized to detect areas at risk of desertification in North China based on spot vegetation imagery. J. Arid Environ. 67, 308–327.

Huete, A.R., 1988. A soil-adjusted vegetation index (ASVI). Remote Sens. Environ. 25, 295–309.

Iqbal, M.F., Khan, I.A., 2014. Spatiotemporal land use land cover change analysis and erosion risk mapping of Azad Jammu and Kashmir, Pakistan. Egypt. J. Remote Sens. Space Sci. 17, 209–229.

Jayanth, J., Koliwad, S., Kumar, T.A., 2015. Classification of remote sensed data using Artificial Bee Colony algorithm. Egypt. J. Remote Sens. Space Sci. 18, 119–126.

Ji, X., Niu, X., 2014. The attribute accuracy assessment of land cover date in the national geography conditions survey. ISPRS Ann. Photogramm. Remote Sens. Spatial Inf. Sci. Vol.II-14.

Keuchel, J., Naumann, S., Heiler, M., Siegmund, A., 2003. Automatic land cover analysis for Tenerife by supervised classification using remotely sensed data. Remote Sens. Environ. 86, 530–541.

Kim, D., Sexton, J.O., Noojipady, P., Huang, C., Anand, A., Channan, S., Feng, M., Townshend, J.R., 2014. Global, Landsat-based forest-cover change from 1990 to 2000. Remote Sens. Environ. 155, 178–193.

Li, H., Xie, Y., Yu, L., Wang, L., 2011. A study on the land cover classification of arid region based on Multi-temporal TM images. Procedia Environ. Sci. 10, 2406–2412.

Li, P., Jiang, L., Feng, Z., 2014. Cross-comparison of vegetation indices derived from Landsat-7 Enhanced Thematic Mapper Plus (ETM +) and Landsat-8 operational land imager (OLI) sensors. Remote Sens. 6, 310–329. http://dx.doi.org/10.3390/rs6010310.

MLWE, 2012. Eritrea's Five Years Action Plan. For the Great Green Wall Initiative (GGWI) Draft, Department of Environment, (2011–2015), Asmara, Eritrea, pp. 3–12.

Ma, Z., Xie, Y., Jiao, J., Li, L., Wang, X., 2011. The construction and application of an Albedo-NDVI based desertification monitoring model. Procedia Environ. Sci. 10, 2029–2035.

McFeeters, S.K., 1996. The use of normalized difference water index (NDWI) in the delineation of open water features. Int. J. Remote Sens. 17, 1425–1432.

MOA, 2002. The National Action Programme for Eritrea to Compact Desertification and Mitigate the Effects of Drought. Asmara, Eritrea, (pp. 20-72 & 179). http://www.unccd.int/ActionProgrammes/eritrea-eng2002.pdf.

Naqvi, H.R., Siddiqui, L., Devi, L.M., Siddiqui, M.A., 2014. Landscape transformation analysis employing compound interest formula in the Nun Nadi Watershed, India. Egypt. J. Remote Sens. Space Sci. 17, 149–157.

Nyssen, J., Poesen, J., Moeyersons, J., Deckers, J., Haile, M., Lang, A., 2004. Human impact on the environment in the Ethiopian and Eritrean highlands-a state of the art. Earth Sci. Rev. 64, 273–320.

Papa, J.P., Falcao, A.X., Albuquerque, V.H.C., Tavares, J.M.R.S., 2012. Efficient supervised optimum-path forest classification for large datasets. Pattern Recogn. 45, 512–520.

Petta, R.A., Carvalho, L.V., Erasmi, S., Jones, C., 2013. Evaluation of desertification processes in serido region (NE Brazil). Int. J. Geosci. 4, 12–17.

Puyavaud, J.P., 2003. Short communication standardizing the calculation of the annual rate of deforestation. For. Ecol. Manage. 177, 593–596.

Rawat, J.S., Biswas, V., Kumar, M., 2013. Changes in land use/cover using geospatial techniques: a case study of Ramnagar town area, district Nainital, Uttarakhand, India. Egypt. J. Remote Sens. Space Sci. 16, 111–117.

Rawat, J.S., Kumar, M., 2015. Monitoring land use/cover change using remote sensing and GIS techniques: a case study of Hawalbagh block, district Almora, Uttarakhand, India. Egypt. J. Remote Sens. Space Sci. 18, 77–84.

Sexton, J.O., Urban, D.L., Donohue, M.J., Song, C., 2013. Long-term land cover dynamics by multi-temporal classification across the Landsat-5 record. Remote Sens. Environ. 128, 246–258.

Shan-long, L., Xiao-hua, S., Le-jun, Z., 2006. Land cover change in Ningbo and its surrounding area of Zhejiang Province, 1987–2000. J. Zhejiang Univ. Sci. A 7 (4), 633–640.

Sumit Chakravarty, S.K., Ghosh, C.P., Suresh, A.N., Dey, Gopal Shukla, 2012. Deforestation: Cause, Effect and Control Strategies, Global Perspectives on Sustainable Forest Management, Dr. Clement A Okia (Ed.), ISBN: 978-953-51-0596-5, InTech. pp. 1–27.

Teklay, M., 1999. Earth science education in Eritrea. J. Afr. Earth Sc. 28 (4), 805–810.

Torahi, A.A., Rai, S.C., 2011. Land cover classification and forest change analysis using satellite imagery – a case study in Dehdez area of Zagros Mountain in Iran. J. Geogr. Inf. Syst. 3, 1–11.

Tucker, C.J., Townshend, J.R.G., 2000. Strategies for monitoring tropical deforestation using satellite data. Int. J. Remote Sens. 21 (6 & 7), 1461–1471.

Waal, A.D., 1991. Thirty Years of War and Famine in Ethiopia. Evil Days, New York, Human Rights Watch, an African Watch Report http://www.hrw.org/sites/default/files/reports/Ethiopia919.pdf.

Xu, H., 2006. Modification of normalized difference of water index (NDWI) to enhance open water features in remotely sensed imagery. Int. J. Remote Sens. 27, 3025–3033.

Yang, X., Yang, T., Ji, Q., He, Y., Ghebrezgabher, M.G., 2014. Regional-scale grassland classification using moderate-resolution imaging spectrometer datasets based on multistep unsupervised classification and indices suitability analysis. J. Appl. Remote Sens. 8 (1). http://dx.doi.org/10.1117/1.JRS.8.083548.

Yiran, G.A.B., Kusimi, J.M., Kufogbe, S.K., 2012. A synthesis of remote sensing and local knowledge approaches in land degradation assessment in the Bawku East District, Ghana. Int. J. Appl. Earth Obs. Geoinf. 14, 204–213.

Yuan, F., Sawaya, K.E., Loeffelholz, B.C., Bauer, M.E., 2005. Land cover classification and change analysis of the twin cities (Minnesota) metropolitan area by multitemporal landsat remote sensing. Remote Sens. Environ. 98, 317–328.

Zhang, X., Delu, P., Chen, J., Zhan, Y., Mao, Z., 2013. Using long time series of Landsat data to monitor impervious surface dynamics a case study in the Zhoushan Islands. J. Appl. Remote Sens. 7. http://dx.doi.org/10.1117/IJRS.7.073515.